



Universidad Autónoma  
de Madrid

**Biblos-e Archivo**  
Repositorio Institucional UAM

Repositorio Institucional de la Universidad Autónoma de Madrid  
<https://repositorio.uam.es>

Esta es la **versión de autor** del artículo publicado en:  
This is an **author produced version** of a paper published in:

Applied Catalysis B: Environmental 293 (2021): 120235

**DOI:** <https://doi.org/10.1016/j.apcatb.2021.120235>

**Copyright:** © 2021 Elsevier B.V. This manuscript version is made available under the CC-BY-NC-ND 4.0 licence <http://creativecommons.org/licenses/by-nc-nd/4.0/>

El acceso a la versión del editor puede requerir la suscripción del recurso  
Access to the published version may require subscription

1 Palladium-based Catalytic Membrane Reactor  
2 for the continuous flow hydrodechlorination of  
3 chlorinated micropollutants

4  
5 *Julia Nieto-Sandoval\**, *Esther Gomez-Herrero*, *Macarena Munoz\**, *Zahara M. de Pedro*  
6 *and Jose A. Casas*

7 Chemical Engineering Department, Universidad Autónoma de Madrid, Ctra. Colmenar  
8 km 15, 28049 Madrid, Spain

9 \*Corresponding authors phones: +34 91 497 3425, +34 91 497 3991; e-mails: [julia.nieto-](mailto:julia.nieto-sandoval@uam.es)  
10 [sandoval@uam.es](mailto:sandoval@uam.es), [macarena.munnoz@uam.es](mailto:macarena.munnoz@uam.es)

## **Abstract**

This work is focused on the development of a Pd-based catalytic membrane reactor (Pd/CMR) for its application in continuous flow hydrodechlorination (HDC) of chlorinated micropollutants. A cylindrical inert porous alumina membrane was decorated on the outer with well-dispersed Pd nanoparticles (0.2% wt.). The Pd/CMR was fully characterized by different techniques. The catalytic system was applied for the degradation of the persistent anti-inflammatory drug diclofenac (DCF) under ambient conditions. A remarkable stability was observed upon long-term HDC reaction, with a reasonable DCF conversion (60%). Notably, as the process could be described by pseudo-first order kinetic, the initial concentration did not affect the final conversion achieved. Finally, the versatility of the system was successfully demonstrated using a real aqueous matrix (tap water). All in all, Pd/CMR exhibited a remarkable feasibility for the implementation of the HDC technology on a larger scale, showing an extraordinary catalytic performance for up to 200 h.

## **Keywords**

Catalytic hydrodechlorination; Diclofenac; Catalytic membrane reactor; Pd-structured catalysts; Drinking water treatment.

## 1. Introduction

Drinking water is of vital importance for life on Earth. With the advancement of technology and industrial growth, freshwater resources are threatened, and waste discharges may cause contamination problems by emerging pollutants. Among them, the organochlorinated ones are particularly hazardous since they are not completely eliminated in conventional treatment plants due to their low biodegradability and high toxicity [1, 2]. Furthermore, they exhibit high persistence in the aquatic environment and thus, in common drinking water sources like rivers, lakes or reservoirs, which may ultimately generate important human risks [3, 4].

In the last few years, catalytic hydrodechlorination (HDC) has emerged as a promising solution for the removal of organochlorinated micropollutants in drinking water treatment [5-7]. HDC is a low-energy and environmentally-friendly technology capable of transforming chlorinated organics into less harmful hydrogenated products and thus, it is able to significantly reduce the effluent ecotoxicity [8, 9]. HDC consists in a reaction usually catalyzed by precious metals under ambient conditions, where hydrogen reacts with the chlorinated compound and leads to the production of an organic chlorine-free product together with HCl [10].

Among the metals used as active phase in the catalysts employed for liquid-phase HDC reaction, palladium (Pd) is considered the most suitable one due to its inherent capacity to dissociate hydrogen and promote C-Cl bond scission [11-13]. Furthermore, Pd shows a high resistance to the corrosive effects of the HCl generated along reaction, one of the main phenomena associated with catalyst deactivation [14, 15], together with the adsorption of chlorinated species and by-products and chemical poisoning through Pd-Cl interactions [16, 17]. The choice of the catalyst support can also impact the activity and stability of the resulting catalyst to a high extent [18, 19]. In this sense, inert materials

like alumina, ceria and zirconia appear as excellent supports for Pd immobilization [7, 18, 20]. Among them, alumina stands out due to its strong interaction with supported Pd leading to high metal dispersion, and its high mechanical resistance [11, 21].

Up to now, the application of HDC for chlorinated micropollutants removal has been successfully performed at lab scale by conventional catalytic processing (*i.e.* slurry batch reactors) using powdered Pd/Al<sub>2</sub>O<sub>3</sub> catalysts [5, 22]. Nevertheless, this configuration does not allow optimizing hydrogen consumption, and the microenvironment created by the solid-liquid-gas interface cannot be controlled. Apart from these issues, the potential application of this technology at larger scales must consider that operation will take place under very demanding conditions: continuous operation, diluted streams, non-steady conditions, and high removal efficiency. The use fixed bed reactors packed with granular catalysts appear as an interesting option for the application of HDC but they can result in large pressure drops and suffer the risk of blockage [23, 24] [25] [26]. On the other hand, uniform flow and optimal mixing are also important challenges in this kind of system [27, 28].

Catalytic Membrane Reactors (CMRs) offer unprecedented advantages for continuous-flow HDC. CMR owns a self-supported three-dimensional cylindrical structure which acts as support for the active phase as well as an interface between hydrogen and the aqueous phase [29]. Hydrogen permeates through the porous material to the external membrane surface, where a controlled reaction zone is formed to favor the three-phase contact (aqueous micropollutant solution- solid catalyst-hydrogen gas). This unique configuration allows continuous HDC treatment and offers significant advantages in terms of cost, design and manufacture compared with current technologies. Pd nanoparticles can be in-situ synthesized just on the external surface, allowing simple manufacture and savings in metal consumption. To best of our knowledge, CMR

application in HDC treatment have not been investigated so far. However, several successful attempts can be found for three-phase hydrogenation reactions using Catalytic Membrane Reactors that acted as liquid/gas phase contactor and as support for a solid catalyst [30-33]. Moreover, other catalytic processes such as phenol oxidation with in-situ generated hydrogen peroxide [34] and photocatalytic oxidation of diclofenac applied this type of structured catalysts [35].

Herein, the preparation and application of a Pd/CMR in continuous-flow HDC has been investigated. A porous alumina membrane tube was used as support material. The optimization of the Pd/CMR preparation was firstly addressed following a procedure which included ion adsorption of a palladium solution, microwave drying, calcination and reduction stages. The resulting Pd/CMR was fully characterized by a wide range of techniques, which allowed to confirm the successful homogeneous decoration of the membrane surface by Pd nanoparticles of small sizes and narrow distribution. Its application in continuous-flow HDC was tested using the anti-inflammatory drug diclofenac (DCF) as target pollutant given its high persistence and widespread occurrence in the aquatic environment [36, 37]. The catalytic performance was assessed in long-term operation under continuous mode for up to 200 h. The impact of the main variables of the process *i.e.* flow rate and DCF initial concentration were systematically evaluated. Finally, the versatility of the system was validated using a real aqueous matrix (tap water).

## **2. Materials and methods**

### **2.1 Materials**

Diclofenac sodium salt (analytical standard), 2-anilinophenylacetic acid (88%) and palladium (II) chloride (anhydrous, 60%) were supplied by Sigma-Aldrich. Hydrochloric

acid (37%) and acetic acid (99.5%) were provided by Panreac and acetonitrile (99.9%) by Scharlau. Hydrogen (99.999%) was delivered by Praxair. The experiments were carried out using deionized water, unless otherwise indicated.

## *2.2 Palladium-based Catalytic Membrane Reactor preparation and characterization*

Commercial porous alumina membrane tubes (Likuid Nanotek) were used as the starting material for the preparation of the Pd/CMR. Cylindrical pieces of 80 mm in length and 11 g of weight were used. Their mean outside and internal diameters were 10 and 6 mm, respectively. The average porous size of the membrane was 5.5  $\mu\text{m}$ .

The Pd/CMR was prepared by the ion-adsorption technique using a concentrated aqueous solution of palladium chloride (51 g L<sup>-1</sup>). Porous membranes capped at one end were immersed in 18 mL of the solution at pH=1 (using HCl) for 2 h, which favors the adsorption of Pd by ion exchange due to the protonation of alumina support positively charged [38, 39]. A N<sub>2</sub> flow was fed inside the tube to promote Pd impregnation only onto the outer surface of the membrane avoiding further penetration into the pore structure as well as to avoid possible membrane pore blocking. Afterwards, Pd/CMRs were microwave dried for 10 min. To warrant a homogenous dispersion of Pd, the tube was periodically rotated. The obtained materials were left for 2 h at 60 °C. In preliminary studies, the number of ion-adsorption cycles to achieve the desired load of Pd load was analyzed. In this case, five consecutive ion-adsorption cycles were required to achieve significant Pd load. The dried membranes were finally submitted to consecutive thermal treatments of calcination at 300 °C in air atmosphere for 4 h and reduction in H<sub>2</sub> (100 N mL min<sup>-1</sup>) at 150 °C for 2 h.

In order to characterize the Pd/CMR catalyst a cross-section piece was cut before and after its use. The textural properties of the Pd/CMR, previously outgassed overnight at 150 °C to a residual pressure of  $<10^{-3}$  Torr, were characterized by nitrogen adsorption–desorption at  $-196$  °C using a Micromeritics Tristar 3020 apparatus. The Pd content was determined by Inductively Coupled Plasma Mass Spectrometry (ICP-MS) using a NexION 300 X Perkin Elmer instrument. Elemental analyses of the fresh and used catalysts were carried out in a LECO CHNS-932 Elemental Analyzer. Transmission electron microscopy (TEM) images of the fresh and used Pd/CMR were obtained using a JEOL JEM 2100 microscope. The software “ImageJ” was used for measuring and counting the palladium nanoparticles on digital TEM images (more than 200 nanoparticles were measured per sample). Additional images of the CMR were obtained by a Nikon Eclipse Ci-S / Ci-L optical microscope equipped with a DS-Fi2 digital camera and a DS-U3 control unit. The X-ray photoelectron spectroscopy (XPS) was employed to determine the surface Pd species in the catalyst, using a spectrometer PHI VersaProbe II equipped with a Al K $\alpha$  X-ray excitation source, 1486.6 eV. The software XPS-Peak was used for peaks deconvolution and the area of the spectral peaks was used to calculate the surface Pd species ratio. The crystalline phases were analysed by X-ray diffraction (XRD) using a Bruker D8 diffractometer. The thermal stability of the Pd/CMR was also evaluated by thermogravimetric analyses in air using a TA instruments SDT650 apparatus.

### *2.3 Experimental procedure*

Aqueous-phase HDC reactions were performed in a double jacketed glass tube reactor continuously fed in up-flow mode with an inlet aqueous stream of 0.2 mL min $^{-1}$  (100  $\mu$ g L $^{-1}$  DCF) at 25 °C. The Pd/CMR was situated at the center of the tube reactor. A H $_2$  flow was continuously fed inside the membrane, which warranted the flow of the reagent from



the core of the membrane to the catalytically active sites at the external surface, as is shown in Fig. 1.

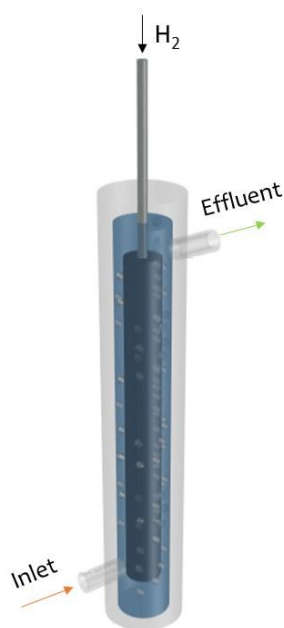


**Fig. 1.** Experimental set up of the long-term HDC reaction.

The performance of the Pd/CMR was evaluated in a long-term continuous experiment (with up to 200 h time on stream). The main variables of the system *i.e.* initial DCF concentration ( $100 - 500 \mu\text{g L}^{-1}$ ) and feed flow rate ( $0.1$  and  $0.2 \text{ mL min}^{-1}$ ) were evaluated. The versatility of the system was finally assessed using a real aqueous matrix representative for the application of HDC in drinking water treatment *viz.* tap water.

Liquid samples were periodically withdrawn from the reactor and analyzed. DCF and the organic reaction products concentrations were quantified by HPLC-UV (Prostar, Varian model 410) using an Eclipse Plus C18 column (15 cm length, 4.6 mm diameter) (Agilent) as stationary phase. The analyses were carried out at 270 nm using a 57/43% (v/v) mixture of acetonitrile and acetic acid aqueous solution (75 mM) as the mobile phase. The intermediate, 2-(2-chloroanilino)-phenylacetate (Cl-APA), and the reaction product, 2-

anilinophenylacetate (APA), were identified in a previous work by liquid chromatography-mass spectrometry [40].

### 3. Results and Discussion

#### 3.1 Pd/CMR characterization

Pd/CMR was fully characterized by different techniques. Fig. 2 shows the images of the Pd/CMR after the different steps of the catalyst preparation (fresh material, ion-adsorption, calcination and reduction). As can be observed, the color of the CMR surface evolved after each catalyst preparation step from white to dark orange and, finally, dark grey. The latter color is typical of a surface covered by Pd nanoparticles in which the reduced species Pd(0) is present [41]. According to the optical microscopy images, a homogeneous coating of the CMR surface was apparently achieved. Furthermore, the Pd/CMR cross-section images allowed to confirm that Pd was only deposited onto the outside surface of the CMR.

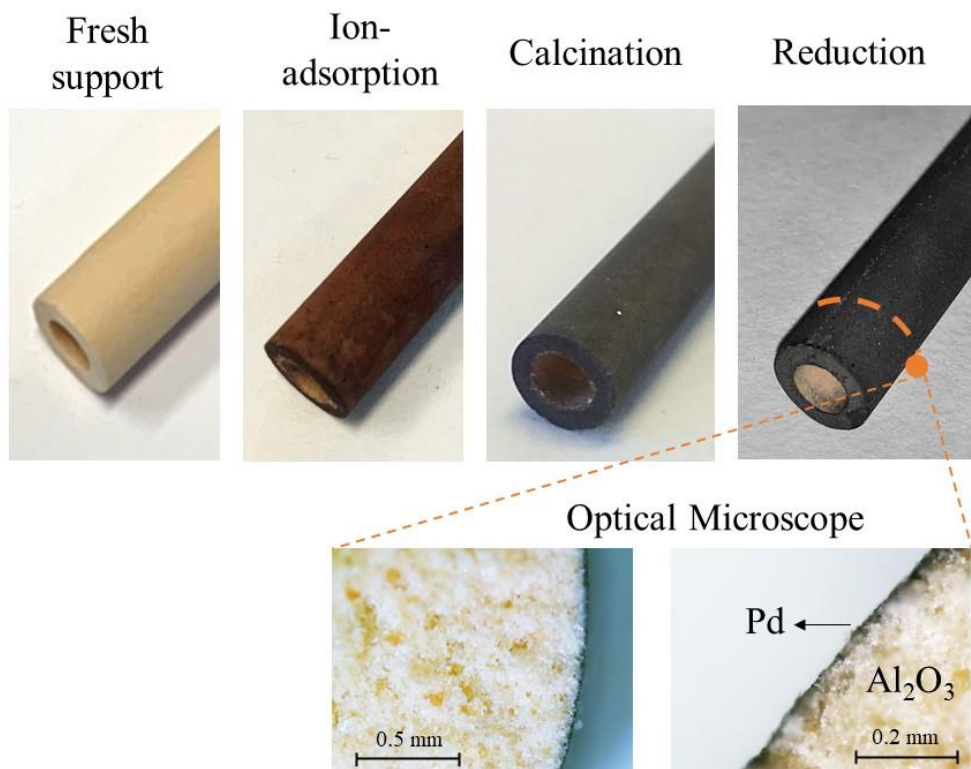


**Fig. 2.** Images of the CMR after the consecutive steps of the preparation procedure. The inset shows cross-section images (optical microscopy) of the final Pd/CMR.

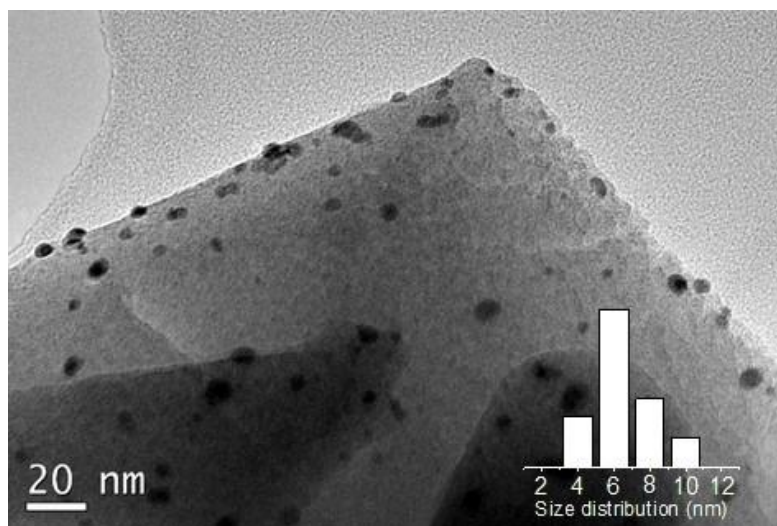


**Fig. 3.** TEM image of the Pd/CMR.

The physicochemical properties of the Pd/CMR catalyst are collected in Table 1. The surface of the Pd/CMR was homogeneously covered by a thin layer of Pd nanoparticles,

with a mean size of  $6 \pm 1.6$  nm, as shown in the TEM image (Fig. 3). The ICP-MS analysis allowed to confirm a Pd loading in the catalyst close to 0.2% wt. Nevertheless, since the Pd active phase was only present in the outer surface of the CMR, the content of Pd revealed by XPS analysis was considerably higher (13% wt.). The core-level spectrum of Pd 3d is given in Fig. 4. The zerovalent ( $\text{Pd}^0$ ) and electrodeficient ( $\text{Pd}^{n+}$ ) palladium bands were centered at binding energy values of 334.8 eV and 340.1 eV, corresponding to Pd  $3d_{5/2}$  and Pd  $3d_{3/2}$ , respectively [42]. The  $\text{Pd}^0/\text{Pd}^{n+}$  ratio calculated was  $1.03 \pm 0.05$ , being 1.0 the optimum ratio determined for the higher activity of Pd catalysts during HDC reactions [43]. The XRD pattern of the alumina membrane support confirmed its crystalline nature. Nevertheless, the low palladium content together with its homogeneous distribution did not allow to clearly differentiate the palladium present in the Pd/CMR (see Fig. S1 of the Supplementary Material for experimental data).

**Table 1.** Main characteristics of the Pd/CMR.

Catalyst	Pd (% wt.)	dp (nm)	BET ( $\text{m}^2 \text{g}^{-1}$ )	Density ( $\text{g cm}^{-3}$ )	$\text{Pd}^0/\text{Pd}^{n+}$
Pd/CMR	0.2	$6 \pm 1.6$	3	1.61	1.03

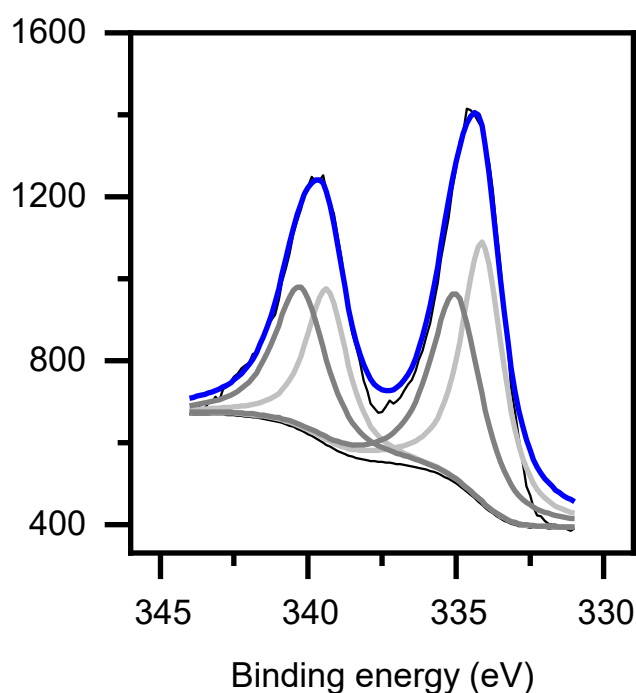


**Fig. 4.** Deconvolution of the Pd 3d core-level spectra of the Pd/CMR fresh catalyst.

### *3.2 Application of Pd/CMR in continuous-flow HDC*

Fig. 5 shows the results obtained upon long-term HDC of DCF at 25 °C with the Pd/CMR developed in this work. As can be observed, DCF concentration in the reactor effluent remained constant achieving a conversion value around 64% during the whole time on stream (120 h). The catalyst stability was evaluated at such conversion to observe possible deactivation from its beginning. Nevertheless, the optimization of the operating conditions could lead to the complete removal of DCF and the chlorinated intermediate. As shown in a previous work, the HDC of DCF proceeds according to a consecutive reaction pathway where DCF reacts with hydrogen to produce Cl-APA, which is further hydrodechlorinated to APA; this transformation results in a significant abatement of the effluent toxicity [40]. In the current study, both the intermediate and the chlorine-free

final product were detected in the reactor effluent. They showed the same trend as DCF, keeping constant their concentration during the long-term HDC reaction. It must be noted that both carbon and chlorine balances were closed above 95%. A slight decrease in the pH value of the effluent from the initial (pH<sub>0</sub>~6.9) to pH~6.6 was observed due to HCl release during the HDC of DCF. Nevertheless, this effect did not affect the catalyst stability, which is consistent with a previous work for the HDC of DCF using a powdered Pd/Al<sub>2</sub>O<sub>3</sub> catalyst and operating in batch mode [40].

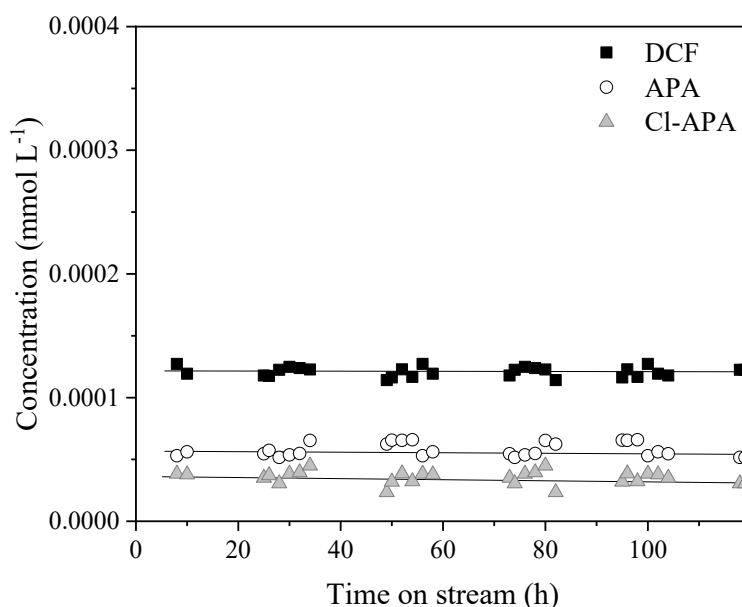


**Fig. 5.** Evolution of DCF, Cl-APA and APA upon long-term HDC reaction with Pd/CMR system ([DCF]<sub>0</sub> = 0.00034 mmol L<sup>-1</sup>; H<sub>2</sub> = 50 N mL min<sup>-1</sup>; Q = 0.2 mL min<sup>-1</sup>; 25 °C).

The high stability of the Pd/CMR was further confirmed by the characterization of the used solid. The elemental analysis demonstrated that Pd/CMR did not suffer any sign of fouling (neither by the reactant nor by the intermediate or product) since the carbon content remained unchanged after the HDC reaction (0.12% wt.). In the same line, the thermogravimetric analysis revealed that the structured catalyst did not change its weight in the temperature range of 30 – 900 °C (see Fig. S2 of the Supplementary Material). On

the other hand, the Pd content remained unchanged after the treatment, which allows to discard possible metal leaching. In fact, TEM images of the Pd/CMR after the long-term continuous experiment also showed Pd nanoparticles homogeneously distributed on the CMR surface with an average size of 6 nm (see Fig. S3 of Supplementary Material). Furthermore, the  $\text{Pd}^0/\text{Pd}^{n+}$  ratio of the used Pd/CMR was  $0.96 \pm 0.05$  (see Fig. S4 of the Supplementary Material), which is similar to the fresh Pd/CMR. No signs of damage in the Pd/CMR can be observed after its use (see Figure S5 of the Supplementary Material).

The results obtained in this work can be favorably compared with those previously reported in the literature for the treatment of organochlorinated pollutants by HDC using powdered catalysts [5, 7, 44, 45], since that configuration results a challenge for catalyst recovery and reusability operating in continuous mode and can also lead to high pressure drops. Although long-term application of this technology has been scarcely investigated,  $\text{H}_2$  transfer limitations and loss of catalytic activity appear as important limitations [46]. Xiong et al. (2018) implemented a novel Pd/CNTs-Ni foam composite catalyst for the HDC of chlorophenols in continuous-flow under ambient conditions, showing high efficiency at short residence times and excellent catalytic stability after 60 h. Nevertheless, the HDC activity was sensitive to the Pd particle size and the reaction was limited by  $\text{H}_2$  mass transfer limitations [42]. More recently, Luo et al. (2020) showed more promising results in this context with the developed of a continuous system based on the deposition of Pd nanoparticles on  $\text{H}_2$  transfer hollow-fiber membranes for the dechlorination of 1,1,1-trichloroethane and trichloroethene, achieving high conversions and overcoming one of the principles limitations, the catalyst loss, since just 4% of Pd was lost over 90 days of continuous operation [46]. Thus, this work presents a novel system using a Pd-based CMR easily prepared that avoid pressure drops issues and  $\text{H}_2$  mass transfer limitations. Although operating conditions could be optimized to increase

DCF conversion, the main goal of this work was to demonstrate the outstanding stability of the catalytic system.

### 3.3 Operating conditions study

It must be noted that the reactor was operated at steady-state conversions under continuous mode; therefore, different operating conditions were tested to evaluate activity and stability by directly modifying the inlet stream. It was kept operating 25 h of time on stream in each experiment.

The concentration of micropollutants in a drinking water treatment plant (DWTP) can suffer important variations. Accordingly, it is essential to analyze the effect of the initial pollutant concentration on the performance of the Pd/CMR system. For such goal, DCF concentration was varied from 100 to 500  $\mu\text{g L}^{-1}$  (0.00034 to 0.00169  $\text{mmol L}^{-1}$ ). According to the obtained results (Fig. 6) all the experiments resulted in similar conversion values, in the range of 58% to 64%. The high activity of the Pd/CMR regardless the pollutant concentration is an important feature for the potential application of HDC as polishing step in DWTPs.

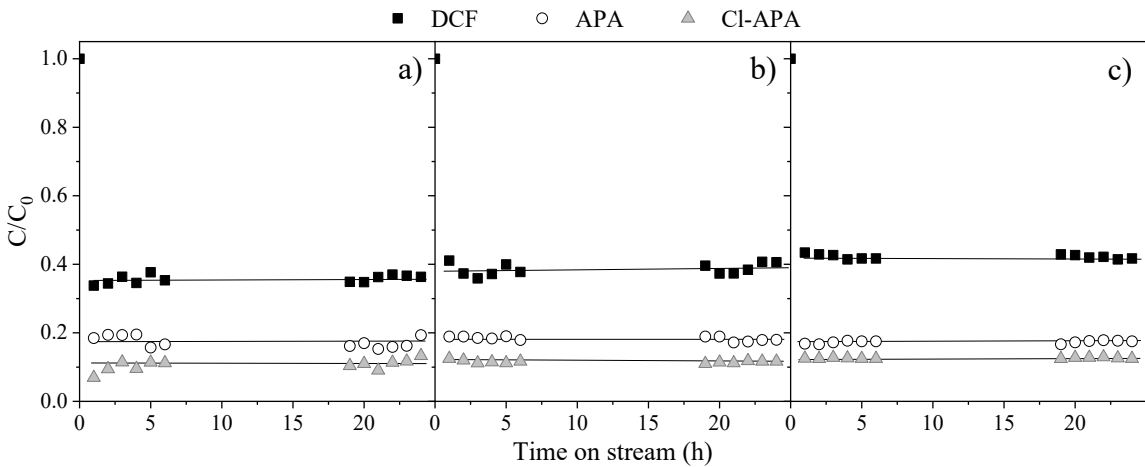




**Fig. 6.** Evolution of DCF, intermediate and product upon long-term HDC reaction with Pd/CMR system at initial DCF concentrations of a) 0.00034 mmol L<sup>-1</sup>, b) 0.00068 mmol L<sup>-1</sup> and c) 0.00169 mmol L<sup>-1</sup> (H<sub>2</sub> = 50 N mL min<sup>-1</sup>; Q = 0.2 mL min<sup>-1</sup>; 25 °C).

Considering the above-mentioned results, it can be concluded that the HDC reaction follows first order kinetics as DCF conversion is independent of the initial pollutant concentration. This is in good agreement with the previous literature in HDC [17, 47, 48]. Taking into account that the process takes place under kinetic control and that hydrogen concentration is kept constant during the experiments, an apparent pseudo-first order kinetic equation was applied to calculate the HDC rate constants as follows:

$$\frac{W}{F_{DCF,0}} = \frac{W}{Q \cdot C_{DCF,0}} = \int_0^{X_{DCF}} \frac{dX_{DCF}}{k \cdot C_{DCF,0} \cdot (1 - X_{DCF})} \quad (1)$$

Where  $W$  is the catalyst weight (g),  $Q$  is the feed flow rate (mL min<sup>-1</sup>),  $X_{DCF}$  is the conversion of DCF, and  $k$  is the apparent pseudo-first order rate constant (mL g<sub>cat</sub><sup>-1</sup> min<sup>-1</sup>).

Equation 1 was successfully fitted to the experimental data obtained at the different DCF initial concentrations tested. The HDC rate constant obtained was 1.66 · 10<sup>-2</sup> mL g<sub>cat</sub><sup>-1</sup> min<sup>-1</sup>.

The effect of the feed flow rate on the performance of the system was also investigated. The feed flow rate was decreased to 0.1 mL min<sup>-1</sup> using an initial DCF concentration of 200 µg L<sup>-1</sup> (0.00068 mmol L<sup>-1</sup>). Under these conditions, DCF conversion was significantly increased up to 83% (Fig. 7). This can be explained by the higher space time (V/Q<sub>DCF</sub>) used in this experiment (220 min) compared to the previous ones (110 min). It must be noted that the calculated rate constant was 1.61 · 10<sup>-2</sup> mL g<sub>cat</sub><sup>-1</sup> min<sup>-1</sup>, which is close to the value obtained for the experiment carried out at half initial concentration and twice feed flow rate. These results allowed again to confirm the

flexibility of the system to variable inlet conditions and also to discard external mass transfer limitations [49].

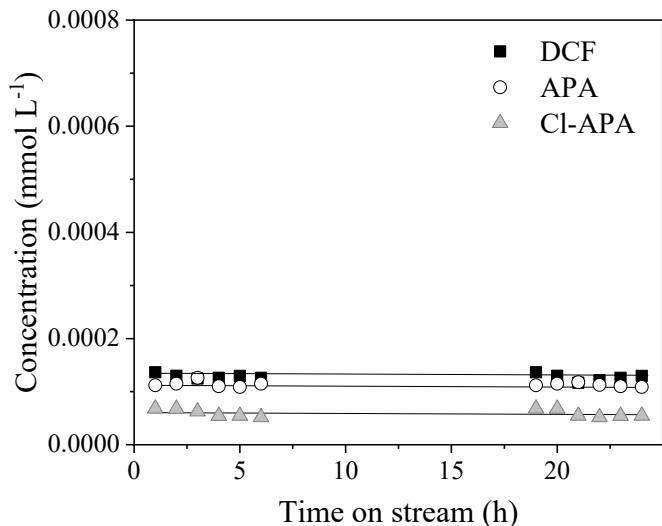


**Fig. 7.** Evolution of DCF, intermediate and product upon long-term HDC reaction with Pd/CMR system at feed flow rate of 0.1 mL min<sup>-1</sup> ([DCF]<sub>0</sub> = 0.00068 mmol L<sup>-1</sup>; H<sub>2</sub> = 50 N mL min<sup>-1</sup>; 25 °C).

One of the main advantages of the Pd/CMR catalysts is that it works as H<sub>2</sub> diffusor and allows to control a reaction zone in the solid-liquid-gas interface, which would optimize the consumption of H<sub>2</sub>. Therefore, a new set of 25 h time on stream experiments has been carried out operating with an inlet aqueous stream of 0.2 mL min<sup>-1</sup> (100 µg L<sup>-1</sup> DCF) at 25 °C and varying the H<sub>2</sub> flow in a range from 10 to 100 N mL min<sup>-1</sup>. Remarkably, DCF conversion remained constant when decreasing the H<sub>2</sub> flow rate up to 10 N mL min<sup>-1</sup>, which demonstrates that it was operated in high excess and it was not a limiting factor at these operating conditions.

### 3.4 Operation in a real water matrix

Pd/CMR has proved to be effective and highly stable in the long-term HDC of DCF during more than 200 h time on stream in deionized water. Nevertheless, this technology is expected to be integrated as a polishing step in the sequential treatment of a DWTP *i.e.* in more complex water matrices. Although the load of pathogens, organic matter and suspended solids would be removed to a high extent prior HDC application, the actual water matrix is far from being deionized water. Clearly, the presence of such species would affect the HDC performance. Consequently, tap water was used as reaction matrix in the inlet stream of the Pd/CMR system for another 25 h time on stream to check its possible impact on its activity and stability. Briefly, the total organic carbon content, inorganic carbon and chloride ion concentrations in the tap water were 2.5, 2.9 and 8.7 mg L<sup>-1</sup>, respectively. The conductivity was 67  $\mu\text{S cm}^{-1}$  and the pH value of 7.2.

Fig. 8 shows the results obtained in the HDC of DCF in tap water using the Pd/CMR system. As can be observed, the concentration of DCF, Cl-APA and APA remained constant along the 25 h time on stream, confirming the extraordinary stability of the catalytic system for more than 220 h in operation. Moreover, DCF conversion was again 60%, which is practically the same as the achieved in deionized water. This finding is of particular importance, as the presence of organic matter in the real water matrix could be a cause of catalyst fouling [47]. In the same line, the presence of inorganic carbon and salts did not lead to any decrease of activity by competitive effects. In fact, the neutralization of the chloride ions generated along reaction by those species could even lead to slightly higher HDC activity [5].

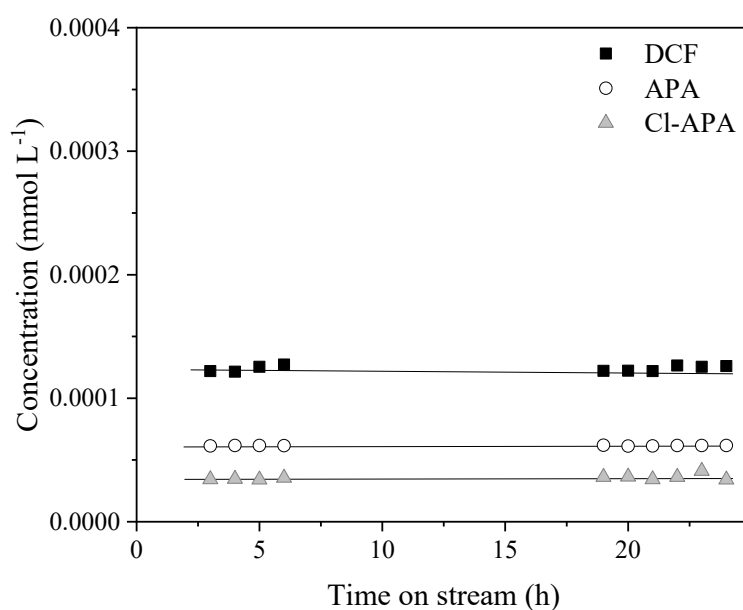


**Fig. 8.** Evolution of DCF, intermediate and product upon long-term HDC in tap water matrix ( $[DCF]_0 = 0.00034 \text{ mmol L}^{-1}$ ;  $H_2 = 50 \text{ N mL min}^{-1}$ ;  $Q = 0.2 \text{ mL min}^{-1}$ ;  $25^\circ\text{C}$ ).

#### 4. Conclusions

The Pd-based Catalytic Membrane Reactor (Pd/CMR) developed in this work has proved to be a highly active, stable and robust catalytic system for continuous-flow HDC. The preparation of the Pd/CMR involved different stages *i.e* ion-adsorption, microwave drying, calcination and reduction, which were carefully optimized to achieve the desired Pd load of 0.2% wt and the optimum Pd species ratio. Pd/CMR worked as an interfacial system where the water effluent and  $H_2$  flow were separated by a porous membrane in which surface Pd nanoparticles of small and narrow size were uniformly dispersed, creating a located reaction zone. The Pd/CMR was applied for the degradation of the antiinflammatory drug diclofenac (DCF) upon long-term HDC reaction, showing 60% conversion of the target pollutant, once the steady state was reached, and a notable

stability for 120 h time on stream without significant changes in the solid. Since the conversion at different initial DCF concentration in the range of 100 – 500  $\mu\text{g L}^{-1}$  remained unchanged, a pseudo-first order kinetic could be considered. Moreover, varying the space time (feed flow rate 0.1-0.2  $\text{mL min}^{-1}$ ) and keeping the relation with the initial DCF concentration allowed to discard the external mass transfer limitations, obtaining a rate constant value of  $1.61 \cdot 10^{-2} \text{ mL g}_{\text{cat}}^{-1} \text{ min}^{-1}$ . Finally, the versatility of the system was demonstrated using a real aqueous matrix (tap water) obtaining similar results as in deionized water. Therefore, the feasibility of Pd/CMR for the implementation of the HDC technology on a larger scale has been demonstrated, showing an extraordinary catalytic performance in the long-term operation under continuous mode for up to 200 h.

## Acknowledgments

This research has been supported by the Spanish MINECO thorough the project PCI2020-112013 and by the CM through the project P2018/EMT-4341. J. Nieto-Sandoval thanks the Spanish MINECO for the FPI predoctoral grant (BES-2017- 081346). M. Munoz thanks the Spanish MINECO for the Ramón y Cajal postdoctoral contract (RYC-2016-20648). E. Gomez-Herrero thanks the CM and Programa Operativo de Empleo Juvenil for the postdoctoral contract (PEJD-2019-POST/AMB-15764).

## Table and Figure captions

**Table 1.** Main characteristics of the Pd/CMR.

**Fig. 1.** Experimental set up of the long-term HDC reaction.

**Fig. 2.** Images of the CMR after the consecutive steps of the preparation procedure. The inset shows cross-section images (optical microscopy) of the final Pd/CMR.

376 **Fig. 3.** TEM image of the Pd/CMR.

377 **Fig. 4.** Deconvolution of the Pd 3d core-level spectra of Pd/CMR fresh catalyst.

378 **Fig. 5.** Evolution of DCF, Cl-APA and APA upon long-term HDC reaction ( $[\text{DCF}]_0 =$   
379  $0.00034 \text{ mmol L}^{-1}$ ;  $\text{H}_2 = 50 \text{ N mL min}^{-1}$ ;  $Q = 0.2 \text{ mL min}^{-1}$ ;  $25^\circ\text{C}$ ).

380 **Fig. 6.** Evolution of DCF, intermediate and product upon long-term HDC reaction with  
381 Pd/CMR system at initial DCF concentrations of a)  $0.00034 \text{ mmol L}^{-1}$ , b)  $0.00068 \text{ mmol}$   
382  $\text{L}^{-1}$  and c)  $0.00169 \text{ mmol L}^{-1}$  ( $\text{H}_2 = 50 \text{ N mL min}^{-1}$ ;  $Q = 0.2 \text{ mL min}^{-1}$ ;  $25^\circ\text{C}$ ).

383 **Fig. 7.** Evolution of DCF, intermediate and product upon long-term HDC reaction with  
384 Pd/CMR system at feed flow rate of  $0.1 \text{ mL min}^{-1}$  ( $[\text{DCF}]_0 = 0.00068 \text{ mmol L}^{-1}$ ;  $\text{H}_2 = 50$   
385  $\text{N mL min}^{-1}$ ;  $25^\circ\text{C}$ ).

386 **Fig. 8.** Evolution of DCF, intermediate and product upon long-term HDC in tap water  
387 matrix ( $[\text{DCF}]_0 = 0.00034 \text{ mmol L}^{-1}$ ;  $\text{H}_2 = 50 \text{ N mL min}^{-1}$ ;  $Q = 0.2 \text{ mL min}^{-1}$ ;  $25^\circ\text{C}$ ).

## 388     **References**

- 389     [1] B. McHugh, R. Poole, J. Corcoran, P. Anninou, B. Boyle, E. Joyce, M. Barry Foley, E.  
390     McGovern, The occurrence of persistent chlorinated and brominated organic contaminants in the  
391     European eel (*Anguilla anguilla*) in Irish waters, *Chemosphere*. 79 (2010) 305-313.  
392     <https://doi.org/10.1016/j.chemosphere.2010.01.029>.
- 393     [2] J. Ahmad, S. Naeem, M. Ahmad, A.R.A. Usman, M.I. Al-Wabel, A critical review on organic  
394     micropollutants contamination in wastewater and removal through carbon nanotubes, *J. Environ.*  
395     *Manage.* 246 (2019) 214-228. <https://doi.org/10.1016/j.jenvman.2019.05.152>.
- 396     [3] Y. Luo, W. Guo, H.H. Ngo, Long Duc Nghiem, F.I. Hai, J. Zhang, S. Liang, X.C. Wang, A  
397     review on the occurrence of micropollutants in the aquatic environment and their fate and removal  
398     during wastewater treatment, *Sci. Total Environ.* 473 (2014) 619-641.  
399     <https://doi.org/10.1016/j.scitotenv.2013.12.065>.
- 400     [4] L.P. Padhye, H. Yao, F.T. Kung'u, C. Huang, Year-long evaluation on the occurrence and fate  
401     of pharmaceuticals, personal care products, and endocrine disrupting chemicals in an urban  
402     drinking water treatment plant, *Water Res.* 51 (2014) 266-276.  
403     <https://doi.org/10.1016/j.watres.2013.10.070>.
- 404     [5] J. Nieto-Sandoval, M. Munoz, Z.M. de Pedro, J.A. Casas, Catalytic hydrodechlorination as  
405     polishing step in drinking water treatment for the removal of chlorinated micropollutants, *Sep.*  
406     *Purif. Technol.* 227 (2019) 115717. <https://doi.org/10.1016/j.seppur.2019.115717>.
- 407     [6] K. Wu, X. Qian, L. Chen, Z. Xu, S. Zheng, D. Zhu, Effective liquid phase hydrodechlorination  
408     of diclofenac catalysed by Pd/CeO<sub>2</sub>, *Rsc Ad.* 5 (2015) 18702-18709.  
409     <https://doi.org/10.1039/c4ra16674d>.
- 410     [7] J. Zhou, Y. Han, W. Wang, Z. Xu, H. Wan, D. Yin, S. Zheng, D. Zhu, Reductive removal of  
411     chloroacetic acids by catalytic hydrodechlorination over Pd/ZrO<sub>2</sub> catalysts, *Appl. Catal.*  
412     *B:Environ.* 134-135 (2013) 222-230. <https://doi.org/10.1016/j.apcatb.2013.01.005>.
- 413     [8] C. Schüth, M. Reinhard, Hydrodechlorination and hydrogenation of aromatic compounds over  
414     palladium on alumina in hydrogen-saturated water, *Appl. Catal. B:Environ.* 18 (1998) 215-221.  
415     [https://doi.org/10.1016/S0926-3373\(98\)00037-X](https://doi.org/10.1016/S0926-3373(98)00037-X).
- 416     [9] K. Mackenzie, H. Frenzel, F. Kopinke, Hydrodehalogenation of halogenated hydrocarbons in  
417     water with Pd catalysts: Reaction rates and surface competition, *Appl. Catal. B:Environ.* 63  
418     (2006) 161-167. <https://doi.org/10.1016/j.apcatb.2005.10.004>.
- 419     [10] C. Xia, Y. Liu, S. Zhou, C. Yang, S. Liu, J. Xu, J. Yu, J. Chen, X. Liang, The Pd-catalyzed  
420     hydrodechlorination of chlorophenols in aqueous solutions under mild conditions: A promising  
421     approach to practical use in wastewater, *J. Hazard. Mater.* 169 (2009) 1029-1033.  
422     <https://doi.org/10.1016/j.jhazmat.2009.04.043>.
- 423     [11] F.J. Urbano, J.M. Marinas, Hydrogenolysis of organohalogen compounds over palladium  
424     supported catalysts, *J. Mol. Catal. A Chem.* 173 (2001) 329-345. [https://doi.org/10.1016/S1381-1169\(01\)00157-1](https://doi.org/10.1016/S1381-1169(01)00157-1).
- 426     [12] M.A. Keane, Supported transition metal catalysts for hydrodechlorination reactions,  
427     *ChemCatChem.* 3 (2011) 800-821. <https://doi.org/10.1002/cctc.201000432>.

- 428 [13] E. Díaz, J.A. Casas, ÁF. Mohedano, L. Calvo, M.A. Gilarranz, J.J. Rodríguez, Kinetics of  
429 the hydrodechlorination of 4-chlorophenol in water using Pd, Pt, and Rh/Al<sub>2</sub>O<sub>3</sub> catalysts, *Ind.*  
430 *Eng. Chem. Res.* 47 (2008) 3840-3846. <https://doi.org/10.1021/ie071517n>.
- 431 [14] S. Ordóñez, E. Díaz, F. Diez V., H. Sastre, Regeneration of Pd/Al<sub>2</sub>O<sub>3</sub> catalysts used for  
432 tetrachloroethylene hydrodechlorination, *React. Kinet. Catal. L.* 90 (2007) 101-106.  
433 <https://doi.org/10.1007/s11144-007-5024-5>.
- 434 [15] Z.M. de Pedro, E. Diaz, A.F. Mohedano, J.A. Casas, J.J. Rodriguez, Compared activity and  
435 stability of Pd/Al<sub>2</sub>O<sub>3</sub> and Pd/AC catalysts in 4-chlorophenol hydrodechlorination in different pH  
436 media, *Appl. Catal. B:Environ.* 103 (2011) 128-135.  
437 <https://doi.org/10.1016/j.apcatb.2011.01.018>.
- 438 [16] G. Yuan, M.A. Keane, Catalyst deactivation during the liquid phase hydrodechlorination of  
439 2,4-dichlorophenol over supported Pd: influence of the support, *Catal. Today.* 88 (2003) 27-36.  
440 <https://doi.org/10.1016/j.cattod.2003.08.004>.
- 441 [17] C.B. Molina, A.H. Pizarro, J.A. Casas, J.J. Rodriguez, Aqueous-phase hydrodechlorination  
442 of chlorophenols with pillared clays-supported Pt, Pd and Rh catalysts, *Appl. Catal. B:Environ.*  
443 148 (2014) 330-338. <https://doi.org/10.1016/j.apcatb.2013.11.010>.
- 444 [18] C. Zheng, M. Li, H. Liu, Z. Xu, Complete dehalogenation of bromochloroacetic acid by  
445 liquid phase catalytic hydrogenation over Pd/CeO<sub>2</sub> catalysts, *Chemosphere.* 239 (2020) 124740.  
446 <https://doi.org/10.1016/j.chemosphere.2019.124740>.
- 447 [19] G. Yuan, M.A. Keane, Liquid phase hydrodechlorination of chlorophenols over Pd/C and  
448 Pd/Al<sub>2</sub>O<sub>3</sub>: A consideration of HCl/catalyst interactions and solution pH effects, *Appl. Catal.*  
449 *B:Environ.* 52 (2004) 301-314. <https://doi.org/10.1016/j.apcatb.2004.04.015>.
- 450 [20] M. Munoz, Z.M. de Pedro, J.A. Casas, J.J. Rodriguez, Improved gamma-alumina-supported  
451 Pd and Rh catalysts for hydrodechlorination of chlorophenols, *Appl. Catal. A:Gen.* 488 (2014)  
452 78-85. <https://doi.org/10.1016/j.apcata.2014.09.035>.
- 453 [21] F. Alonso, I.P. Beletskaya, M. Yus, Metal-mediated reductive hydrodehalogenation of  
454 organic halides, *Chem. Rev.* 102 (2002) 4009-4092. <https://doi.org/10.1021/cr0102967>.
- 455 [22] J. Nieto-Sandoval, E. Gomez-Herrero, F. El Morabet, M. Munoz, Z.M. de Pedro, J.A. Casas,  
456 Catalytic hydrodehalogenation of haloacetic acids: A kinetic study, *Ind. Eng. Chem. Res.* 59  
457 (2020) 17779-17785. <https://doi.org/10.1021/acs.iecr.0c03495>.
- 458 [23] J. Lefevre, M. Gysen, S. Mullens, V. Meynen, J. Van Noyen, The benefit of design of  
459 support architectures for zeolite coated structured catalysts for methanol-to-olefin conversion,  
460 *Catal. Today.* 216 (2013) 18-23. <https://doi.org/10.1016/j.cattod.2013.05.020>.
- 461 [24] A. Avril, C.H. Hornung, A. Urban, D. Fraser, M. Horne, J.-. Veder, J. Tsanaktsidis, T.  
462 Rodopoulos, C. Henry, D.R. Gunasegaram, Continuous flow hydrogenations using novel catalytic  
463 static mixers inside a tubular reactor, *React. Chem. Eng.* 2 (2017) 180-188.  
464 <https://doi.org/10.1039/C6RE00188B>.
- 465 [25] V.I. Simagina, O.V. Netskina, E.S. Tayban, O.V. Komova, E.D. Grayfer, A.V. Ischenko,  
466 E.M. Pazhetnov, The effect of support properties on the activity of Pd/C catalysts in the liquid-  
467 phase hydrodechlorination of chlorobenzene, *Appl. Catal. A:Gen.* 379 (2010) 87-94.  
468 <https://doi.org/10.1016/j.apcata.2010.03.011>.



- 469 [26] A. Koekemoer, A. Luckos, Effect of material type and particle size distribution on pressure  
470 drop in packed beds of large particles: Extending the Ergun equation, *Fuel*. 158 (2015) 232-238.  
471 <https://doi.org/10.1016/j.fuel.2015.05.036>.
- 472 [27] J. Wegner, S. Ceylan, A. Kirschning, Ten key issues in modern flow chemistry, *Chem.*  
473 *Commun.* 47 (2011) 4583-4592. <https://doi.org/10.1039/C0CC05060A>.
- 474 [28] A. Müller, M. Ludwig, M. Arlit, R. Lange, Evaluation of reactor concepts for the continuous  
475 production of fine chemicals using the selective hydrogenation of cinnamaldehyde over palladium  
476 catalysts, *Catal. Today*. 241 (2015) 214-220. <https://doi.org/10.1016/j.cattod.2013.12.051>.
- 477 [29] O. Osegueda, A. Dafinov, J. Llorca, F. Medina, J. Suerias, In situ generation of hydrogen  
478 peroxide in catalytic membrane reactors, *Catal. Today* 193 (2012) 128-136.  
479 <https://doi.org/10.1016/j.cattod.2012.01.040>.
- 480 [30] J.W. Veldsink, Selective hydrogenation of sunflower seed oil in a three-phase catalytic  
481 membrane reactor, *J. Am. Oil Chem. Soc.* 78 (2001) 443-446. [https://doi.org/10.1007/s11746-](https://doi.org/10.1007/s11746-001-0283-2)  
482 [001-0283-2](https://doi.org/10.1007/s11746-001-0283-2).
- 483 [31] G. Bagnato, A. Figoli, C. Ursino, F. Galiano, A. Sanna, A novel Ru–polyethersulfone (PES)  
484 catalytic membrane for highly efficient and selective hydrogenation of furfural to furfuryl alcohol,  
485 *J. Mater. Chem. A*. 6 (2018) 4955-4965 <https://doi.org/10.1039/C7TA10575D>.
- 486 [32] R. Dittmeyer, V. Höllein, K. Daub, Membrane reactors for hydrogenation and  
487 dehydrogenation processes based on supported palladium, *J. Mol. Catal. A Chem.* 173 (2001)  
488 135-184. [https://doi.org/10.1016/S1381-1169\(01\)00149-2](https://doi.org/10.1016/S1381-1169(01)00149-2).
- 489 [33] J.P. Stanford, M.C. Soto, P.H. Pfromm, M.E. Rezac, Aqueous phase hydrogenation of  
490 levulinic acid using a porous catalytic membrane reactor, *Catal. Today*. 268 (2016) 19-28.  
491 <https://doi.org/10.1016/j.cattod.2016.02.026>.
- 492 [34] O. Osegueda, A. Dafinov, J. Llorca, F. Medina, J. Sueiras, Heterogeneous catalytic oxidation  
493 of phenol by in situ generated hydrogen peroxide applying novel catalytic membrane reactors,  
494 *Chem. Eng. J.* 262 (2015) 344-355. <https://doi.org/10.1016/j.cej.2014.09.064>.
- 495 [35] V.C. Sarasidis, K.V. Plakas, S.I. Patsios, A.J. Karabelas, Investigation of diclofenac  
496 degradation in a continuous photo-catalytic membrane reactor. Influence of operating parameters,  
497 *Chem. Eng. J.* 239 (2014) 299-311. <https://doi.org/10.1016/j.cej.2013.11.026>.
- 498 [36] M.O. Barbosa, N.F.F. Moreira, A.R. Ribeiro, M.F.R. Pereira, A.M.T. Silva, Occurrence and  
499 removal of organic micropollutants: An overview of the watch list of EU Decision 2015/495,  
500 *Water Res.* 94 (2016) 257-279. <https://doi.org/10.1016/j.watres.2016.02.047>.
- 501 [37] N. Vieno, M. Sillanpää, Fate of diclofenac in municipal wastewater treatment plant - A  
502 review, *Environ. Int.* 69 (2014) 28-39. <https://doi.org/10.1016/j.envint.2014.03.021>.
- 503 [38] P. Munnik, P.E. de Jongh, K.P. de Jong, Recent Developments in the Synthesis of Supported  
504 Catalysts, *Chem. Rev.* 115 (2015) 6687-6718. <https://doi.org/10.1021/cr500486u>.
- 505 [39] J. Howeizi, S. Taghvaei-Ganjali, M. Malekzadeh, F. Motiee, S. Sahebdehfar, Effect of the  
506 distribution and dispersion of palladium nanoparticles on the reducibility and performance of  
507 Pd/Al<sub>2</sub>O<sub>3</sub> catalyst in liquid-phase hydrogenation of olefins, *Reaction Kinetics, Mechanisms and*  
508 *Catalysis*. 130 (2020) 777-795. <https://doi.org/10.1007/s11144-020-01795-8>.

- 509 [40] J. Nieto-Sandoval, M. Munoz, Z.M. de Pedro, J.A. Casas, Fast degradation of diclofenac by  
510 catalytic hydrodechlorination, *Chemosphere* 213 (2018) 141–148.  
511 <https://doi.org/10.1016/j.chemosphere.2018.09.024>
- 512 [41] W. Chen, L. Zhong, X. Peng, K. Wang, Z. Chen, R. Sun, Xylan-type hemicellulose supported  
513 palladium nanoparticles: a highly efficient and reusable catalyst for the carbon–carbon coupling  
514 reactions, *Catal. Sci. Technol.* 4 (2014) 1426–1435. <https://doi.org/10.1039/C3CY00933E>.
- 515 [42] J. Xiong, Y. Ma, W. Yang, L. Zhong, Rapid, highly efficient and stable catalytic  
516 hydrodechlorination of chlorophenols over novel Pd/CNTs-Ni foam composite catalyst in  
517 continuous-flow, *J. Hazard. Mater.* 355 (2018) 89–95.  
518 <https://doi.org/10.1016/j.jhazmat.2018.05.018>.
- 519 [43] L.M. Gómez-Sainero, X.L. Seoane, J.L.G. Fierro, A. Arcoya, Liquid-Phase  
520 Hydrodechlorination of CCl<sub>4</sub> to CHCl<sub>3</sub> on Pd/Carbon Catalysts: Nature and Role of Pd Active  
521 Species, *J. Catal.* 209 (2002) 279–288. <https://doi.org/10.1006/jcat.2002.3655>.
- 522 [44] J. Nieto-Sandoval, M. Rodriguez, M. Munoz, Z.M. de Pedro, J.A. Casas, Catalyst  
523 deactivation in the hydrodechlorination of micropollutants. A case of study with neonicotinoid  
524 pesticides, *J. Water Process Eng.* 38 (2020) 101550. <https://doi.org/10.1016/j.jwpe.2020.101550>.
- 525 [45] B. Han, W. Liu, J. Li, J. Wang, D. Zhao, R. Xu, Z. Lin, Catalytic hydrodechlorination of  
526 triclosan using a new class of anion-exchange-resin supported palladium catalysts, *Water Res.*  
527 120 (2017) 199–210. <https://doi.org/10.1016/j.watres.2017.04.059>.
- 528 [46] Y. Luo, C. Zhou, Y. Bi, X. Long, B. Wang, Y. Tang, R. Krajmalnik-Brown, B.E. Rittmann,  
529 Long-term continuous co-reduction of 1,1,1-trichloroethane and trichloroethene over palladium  
530 nanoparticles spontaneously deposited on H<sub>2</sub>-transfer membranes, *Environ. Sci. Technol.* (2020).  
531 <https://doi.org/10.1021/acs.est.0c05217>.
- 532 [47] S. Ordóñez, B.P. Vivas, F.V. Díez, Minimization of the deactivation of palladium catalysts  
533 in the hydrodechlorination of trichloroethylene in wastewaters, *Appl. Catal. B: Environ.* 95 (2010)  
534 288–296. <https://doi.org/10.1016/j.apcatb.2010.01.006>.
- 535 [48] M.R. Flid, L.M. Kartashov, Y.A. Treger, Theoretical and applied aspects of  
536 hydrodechlorination processes-Catalysts and technologies, *Catalysts* 10 (2020).  
537 <https://doi.org/10.3390/catal10020216>.
- 538 [49] C. Perego, S. Peratello, Experimental methods in catalytic kinetics, *Catal. Today.* 52 (1999)  
539 133–145. [https://doi.org/10.1016/S0920-5861\(99\)00071-1](https://doi.org/10.1016/S0920-5861(99)00071-1).